Optical transitions of Rh^{2+} in NaCl crystals studied by electron spin resonance and magnetic circular dichroism

H. Vercammen and D. Schoemaker
Department of Physics, University of Antwerp (UIA), Universiteitsplein 1, B-2610 Antwerpen, Belgium

B. Briat and F. Ramaz
Laboratoire d'Optique Physique, École Superieure de Physique et de Chimie Industrielles de la Ville de Paris, 10 rue Vauquelin, 75231 Paris Cedex 05, France

F. Callens
Laboratory for Crystallography and Study of the Solid State, Krijgslaan 281-S1, B-9000 Gent, Belgium
(Received 4 September 1998)

Electron spin resonance, magnetic circular dichroism, and optical absorption spectra of a paramagnetic Rh^{2+} complex are investigated in Rh^{3+} doped solution-grown NaCl single crystals. *x* irradiation of the crystals at 77 K followed by a warm-up to room temperature results in the formation of a stable low-spin Jahn-Teller distorted $RhCl_6^{4-}$ complex possessing D_{4h} symmetry. The unpaired electron is largely localized in the $4d_{z^2}$ orbital of the $Rh^{2+}(4d^7)$ which is involved in a σ type molecular bond with two symmetrically placed Cl^- ions along $\langle 001 \rangle$. The magnetic circular dichroism and optical absorption measurements at 1.4 K reveal two main bands around 12 200 cm^{-1} and 16 200 cm^{-1}. Within the octahedral Tanabe-Sugano formalism of the Rh^{2+} these two absorptions are associated with two vibronically allowed $^2E_g \rightarrow {}^2T_{1g}, {}^2T_{2g}$ molecular transitions. This assignment is in quantitative agreement with the analysis of the **g** matrix components. A small MCD feature at 15 200 cm^{-1} is tentatively associated with two coinciding $^2E_g \rightarrow {}^2T_{1g}, {}^2T_{2g}$ transitions of another, probably a ligand-exchanged, Rh^{2+} center. [S0163-1829(99)00517-2]

I. INTRODUCTION

The Rh^{3+} impurity is a good trap for electrons in the silver halides distinctly influencing the properties of the AgCl and AgBr photographic emulsions. Since these emulsions are precipitated from aqueous solutions, one or more of the halogen ions surrounding the Rh^{3+} ion may be exchanged for, e.g., H_2O molecules, influencing in subtle ways the trapping and stability properties of the resulting Rh^{2+} complex. These changes are of considerable photographic importance. In photographic emulsions of Rh^{3+}-doped AgCl microcrystals, three different Rh^{2+} centers, produced by electron trapping after uv or *x* irradiation have been detected,[1] two of which correspond to aquated forms of the $RhCl_6^{4-}$ complex, $RhCl_4(H_2O)_2^{2-}$ and $RhCl_5(H_2O)^{3-}$, and also a $RhCl_6^{4-}$ complex uncompensated by cation vacancies. Unfortunately, macroscopic single crystals of the silver halides cannot be grown from aqueous solution and as a result no single crystal studies can be performed on singly or multiply aquated rhodium centers in macroscopic AgCl and AgBr crystals. As an alternative system it was decided to perform studies on Rh^{3+} doped NaCl single crystals grown from aqueous solution.

A Rh^{2+} center in solution-grown NaCl has been studied earlier[2] by electron spin resonance (ESR) and the analysis was consistent with a low spin $4d^7$ configuration, in which the unpaired electron is mainly localized in the $Rh^{2+}4d_{z^2}$ orbital. The symmetry of **g** and hyperfine matrices at 77 K was axial along a $\langle 001 \rangle$ direction. At that time, the presence of two symmetrically placed cation vacancies along $\langle 001 \rangle$ was proposed in order to explain the charge compensation and axial symmetry of the ESR spectrum. In a recent paper[3] the center was reexamined, both with ESR and electron nuclear double resonance (ENDOR) and was established to be uncompensated. This Rh^{2+} center, which possesses D_{4h} symmetry, will be referred to as the RTAX center and is the subject of this paper. Rh^{2+} centers with quantitatively quite similar **g** and hyperfine matrices, implying the same $4d_{z^2}$ ground state, were observed in Bridgman-grown[4] AgCl and NaCl single crystals[5] and in solution-grown AgCl microcrystals[1] and NaCl single crystals.[3,6,7]

The optical absorption spectrum of the $Rh^{3+}(4d^6)$ complex in solution is known to consist of two vibronically allowed $d-d$ transitions near 19 300 cm^{-1} and 24 330 cm^{-1} and they were associated with $A_{1g}(t_{2g}^6) \rightarrow {}^1T_{1g}, {}^1T_{2g}(t_g^5 e_g^1)$ transitions.[8] In a recent paper[9] the analogous transitions were found at 18 700 cm^{-1} and 23 750 cm^{-1} in solution-grown Rh^{3+} doped NaCl single crystals. In the same paper it was also reported that a Rh^{2+} optical absorption could be detected in NaCl at 19 350 cm^{-1}, and it was associated, within the octahedral Tanabe-Sugano formalism,[10] with two coinciding $^2E_g(t_{2g}^6 e_g^1) \rightarrow {}^2T_{1g}, {}^2T_{2g}(t_{2g}^5 e_g^2) d-d$ transitions. The Rh^{2+} centers had been produced by heating the NaCl:Rh^{3+} samples to a temperature in the range of 500 °C to 600 °C. From our own optical absorption experiments we know that such a procedure produces many macroscopic scattering centers yielding samples of poor optical quality.

In this paper we will show that Rh^{2+} centers can be produced in a more gentle way yielding NaCl specimens much more suitable for optical experiments. We detect no discern-

ible Rh^{2+} absorption band at 19 350 cm^{-1}, not even by heating or *x* irradiation. By a combination of ESR, optical absorption (OA) and magnetic circular dichroism (MCD) techniques we will establish that the Rh^{2+} RTAX center, possesses several optical absorption bands, the most prominent ones at 12 200 cm^{-1} and 16 200 cm^{-1}, and further a weaker band at $15\,350^{-1}$ and absorptions around $\sim$30 000 cm^{-1}. We will show that within an octahedral Tanabe-Sugano description[10] of the Rh^{2+} ion, the bands at 12 200 cm^{-1} and 16 200 cm^{-1} can be associated with the $^2E_g(t_{2g}^6 e_g^1) \rightarrow {}^2T_{1g}, {}^2T_{2g}(t_{2g}^5 e_g^2)$ transitions mentioned above. The assignments for the other absorptions will be discussed in the text.

II. EXPERIMENTAL

A. Sample preparation

The sodium chloride single crystals used in this study were grown at room temperature by slow evaporation of a saturated aqueous solution of NaCl (Suprapur, Merck), which contained about 0.6 wt. % of the dopant salt $Na_3RhCl_6 \cdot 12H_2O$ (Agfa Gevaert NV). The crystals chosen for measurement were about 10 mm on edge, transparent and pink in color. Irradiation with *x* rays at liquid nitrogen temperature (LNT) followed by suitable optical bleaching and thermal annealing to room temperature was employed to produce the Rh^{2+} species in NaCl.

B. Methods

The ESR spectra were recorded using a Bruker *X*-band spectrometer operating at 9.4 GHz. A continuous flow helium cryostat was mounted in the cavity, so that ESR measurements could be performed in a temperature range from 7 K to 300 K. The ESR correlated optical absorption experiments were performed in the same temperature range with a Varian Cary 5 spectrophotometer employing either a nitrogen bath cryostat or a helium flow cryostat for experiments between 7 K and room temperature.

Details concerning the MCD instrument and the calibration of the spectra are given in Ref. 11. The maximum applied magnetic field was 3 T and all experiments were performed at 1.4 K, the lowest temperature obtainable in the setup. The spectral range ran from 10 000 cm^{-1} in the near IR to the uv around 33 000 cm^{-1}. The MCD correlated optical absorption experiments were performed at 300 K employing a Varian Cary 5E spectrometer and at 1.4 K with a home built double beam attachment to the dichrometer. The crystals were irradiated at 77 K with *x* rays for periods of the order of 20 min. The source was a Siemens *x*-ray tube with a tungsten anticathode, operating at 50 kV and 50 mA. The optical bleachings were performed with a mercury lamp (150 W), together with the appropriate filter combination.

III. EXPERIMENTAL RESULTS

A. Electron spin resonance

No ESR lines were detected in the as-grown NaCl:Rh^{3+} crystals. After *x*-ray irradiation at 77 K and keeping the crystal in the dark, two intense ESR spectra are observed. The high intensity of the first one, the Cl_2^- self-trapped-hole center or V_K center,[12] is indicative for the presence of a highly efficient electron trap in the NaCl lattice, the Rh^{3+} ion in this case. The other strong spectrum is therefore readily associated[7] with a Rh^{2+} center of orthorhombic symmetry. Through ENDOR experiments it is established that this center is accompanied by two next-nearest-neighbor (NNN) cation vacancies symmetrically placed with respect to a {110} plane through the $z \| \langle 001 \rangle$ axis. This Rh^{2+} center will be further on referred to as O(I).

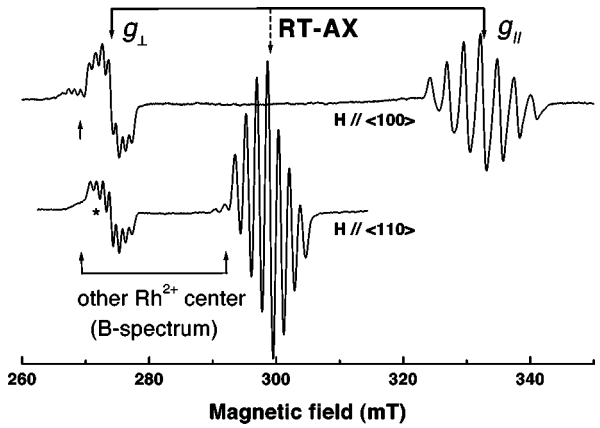

FIG. 1. Rh^{2+} RTAX ESR spectra at 20 K in a Rh^{3+}-doped NaCl solution-grown crystal *x* irradiated at 77 K followed by a long anneal at room temperature. The spectra shown were recorded with the magnetic field along $\langle 100 \rangle$ and $\langle 110 \rangle$. The asterisk denotes the calculated $g_\parallel$ value for the *B* spectrum.

After optical excitation of the *F* center absorption band at[13] 22 340 cm^{-1}, a process which releases mobile electrons in the lattice, the ESR intensity of the rhodium center is only altered to a small extent, but the V_K spectrum decreases in intensity. Heating the sample to 300 K for a few minutes results in the decay of all V_K centers, the formation of a small amount of V_F centers[12] and a small reduction in the Rh^{2+}-center concentration. When the crystal is kept for an hour or more at 300 K, only the Rh^{2+} species remains clearly detectable. During the pulse anneal, the O(I) center is converted around 190 K to a second Rh^{2+} center possessing orthorhombic symmetry. This is the O(II) center with principal **g** matrix axes along the cubic crystal axes and is compensated by only a single cation vacancy in a NNN position. This center is analogous to the dominant Rh^{2+} center in Bridgman-grown NaCl (Ref. 5) and AgCl (Ref. 4). After longer times at room temperature, typically one day or more, the O(II) center in NaCl is converted to the axial Rh^{2+} RTAX center, with the main axis *z* oriented along a cubic direction. This center is identified as being not locally charge compensated.[3] In subsequent ESR and optical experiments the foregoing procedure was shortened to a simple warm-up to room temperature after *x* irradiation at 77 K and an exposure to ambient light. Sometimes this procedure was repeated once or twice in an attempt to enhance the RTAX Rh^{2+} concentration.

The main ESR features of the Rh^{2+} RTAX center have been discussed recently.[3] The properties of the other two Rh^{2+} centers O(I) and O(II) are quite similar. The Rh^{2+} RTAX ESR spectra, for $\mathbf{H} \| \langle 100 \rangle$ and $\langle 110 \rangle$, are presented in Fig. 1. The lines exhibit a well resolved seven line splitting originating from superhyperfine (shf) interaction with

the nuclei of two equivalent Cl^- ($I=3/2$) ions along the $\langle 001\rangle$ oriented symmetry axis z. This points to covalent bonding of the Rh^{2+} with the two Cl^-, thus forming essentially a $RhCl_2$ molecule.

The ESR spectrum is described by the following spin Hamiltonian (usual notation):

$$\mathcal{H}=\mu_B\mathbf{H}\cdot\mathbf{g}\cdot\mathbf{S}+\sum_{i=1}^{2}\mathbf{I}_i\cdot\mathbf{A}\cdot\mathbf{S}; \quad (1)$$

the matrix **A** represents the ^{35}Cl superhyperfine (shf) interaction between **S** ($S=1/2$) and the nuclear spins $\mathbf{I}_1$ and $\mathbf{I}_2$ of the two Cl^- nuclei. The results are presented in Table I.

The behavior of the principal components of the **g** matrix and the strong shf interaction with the chlorine nuclei along the fourfold symmetry axis, confirm the earlier conclusion[2–5] that in the alkali and silver halides the electron is mainly localized in the $4d_{z^2}$ orbital of the Rh^{2+} which forms σ type molecular bonds with two adjoining equivalent Cl^- ions. Recent ENDOR experiments[3] reveal that there is also a much weaker shf interaction with the four equatorial chlorine ligands. From the ESR and ENDOR studies it is concluded that this center consists of a $[RhCl_6]^{4-}$ unit of D_{4h} symmetry, substituting for $[NaCl_6]^{5-}$ without a charge compensating cation vacancy.

The structural assignment of the other Rh^{2+} centers O(I) and O(II) is beyond the scope of this paper and is discussed elsewhere.[3,6,7] Their **g** and **A** matrix principal values are included in Table I for comparison.

Further inspection of the ESR spectrum in Fig. 1 reveals another Rh^{2+} species, formerly denoted as the *B* spectrum[2] and tentatively associated[3] with an aquated form of the $[RhCl_6]^{4-}$ complex, where Cl^- is exchanged by either OH^- or H_2O. From our *X*-band ESR spectra it is very difficult to obtain reliable numerical values of the **g** matrix of this species, but the $g_\perp$ value is surely shifted towards a higher value compared to RTAX. Approximately the same shf structure (seven-line structure) can be discerned, and it is concluded that this complex also contains the same $RhCl_2$ core. A very long time after *x* irradiation (>1 yr) the ESR signal of the *B* spectrum tends to disappear.

An alternative way to produce high Rh^{2+} concentrations is to anneal the crystals to temperatures in the 500–700 °C range. Unlike the *x*-irradiation procedure, the only stable center at room temperature produced by the thermal annealing procedure is identified to be the Rh^{2+} O(II) center associated with a single cation vacancy. Recent ESR and ENDOR studies on Bridgman-grown NaCl crystals[5] have shown that the O(II) center is the most stable center in these crystals too. Thus by annealing solution-grown NaCl:Rh^{3+} crystals to the 500–700 °C range they acquire properties similar to Bridgman-grown crystals.

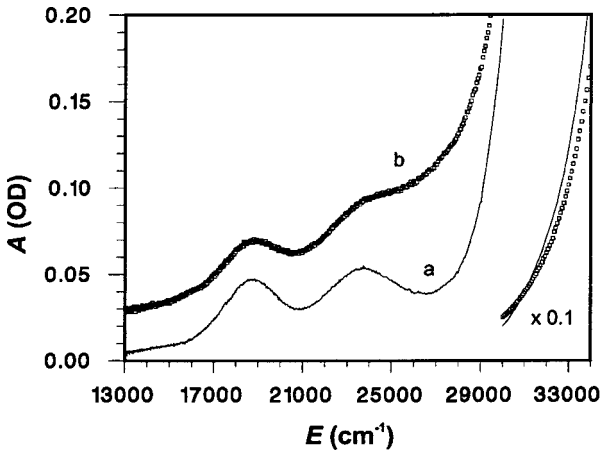

FIG. 2. Optical absorption spectra at 300 K. Curve *a* shows the optical absorption spectrum of the nontreated Rh^{3+}-doped NaCl solution-grown crystal. Curve *b*, which is shifted upwards from curve *a* for clarity, shows the optical absorption spectrum at 300 K of a sample *x* irradiated at 77 K and annealed at room temperature for several days. Both $d-d$ transitions of the Rh^{3+} center are visible at ($18\,700\pm50$) and ($23\,700\pm50$) cm^{-1}, and at higher energy ($\approx30\,000$ cm^{-1}) the charge transfer transition of the Rh^{3+} center.

B. Optical absorption data

The optical absorption spectrum at room temperature of the untreated Rh^{3+} doped NaCl crystals shows (Fig. 2) two broad bands of low intensity at ($18\,700\pm100$) cm^{-1} and ($23\,700\pm100$) cm^{-1} together with a strong charge transfer band of the Rh^{3+} ion beyond $30\,000$ cm^{-1}. The former two broad bands shift roughly 600 cm^{-1} towards higher energies upon cooling to 1.4 K. At the same time the bands sharpen by 20%. For example, the full width at half maximum of the $18\,700$ cm^{-1} band is reduced from 2400 cm^{-1} at 300 K to 2000 cm^{-1} at 1.4 K. It has been proposed[8] in the framework of the octahedral Tanabe-Sugano formalism[10] that the broad bands originate from two weakly allowed $d-d$ transitions within the Rh^{3+}, $^1A_{1g}\rightarrow{}^1T_{1g}, {}^1T_{2g}$, respectively.

In order to produce the Rh^{2+} center the shortened procedure described in the ESR section was applied: *x* irradiation at 77 K followed by a warm-up to room temperature, where

TABLE I. Spin Hamiltonian parameters at 20 K of various Rh^{2+} centers in solution-grown sodium chloride single crystals produced by *x* irradiation. The chlorine hyperfine parameters are expressed in MHz.

Center	g_x	g_y	g_z	$A_x(^{35}Cl)$	$A_y(^{35}Cl)$	$A_z(^{35}Cl)$	Reference
Rh^{2+} O(I) [a]	2.4797_4	2.4712_4	2.0118_8	33.9 ± 0.1	33.9 ± 0.1	72.7 ± 0.2	7,6
Rh^{2+} O(II) [b]	2.4779_4	2.4301_4	2.0154_8	35 ± 1	35 ± 1	73 ± 2	6
Rh^{2+} RTAX [c]	2.4510_1		2.0190_1	33.9 ± 0.1		75.5 ± 0.2	3

[a] $RhCl_6^{4-}$ complex associated with 2 cation vacancies; **g** and **A** matrix axes are along $x\|\langle 110\rangle$, $y\|\langle \bar{1}10\rangle$, and $z\|\langle 001\rangle$.
[b] $RhCl_6^{4-}$ complex associated with 1 cation vacancy; **g** and **A** matrix axes are along the cubic crystal axes.
[c] $RhCl_6^{4-}$ complex nonlocally charge compensated; **g** and **A** matrix axes are along the cubic crystal axes.

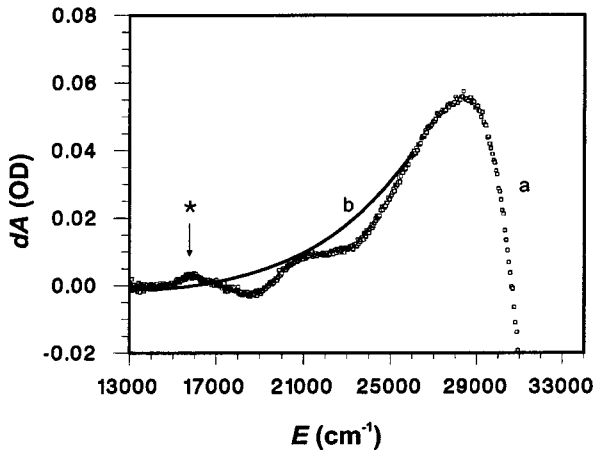

FIG. 3. Differential optical absorption spectra at 300 K. Curve *a* is the difference between traces *a* and *b* of Fig. 2. The solid line *b* is drawn as a guide for the eye: One observes a reduction of the two $d-d$ transition bands of the Rh^{3+} center, the appearance of a relatively strong band around $(28\,500\pm500)$ cm^{-1}, and a weak absorption at 16 000 cm^{-1}, exactly at the position where the MCD demonstrates the occurrence of the major peaks for Rh^{2+}.

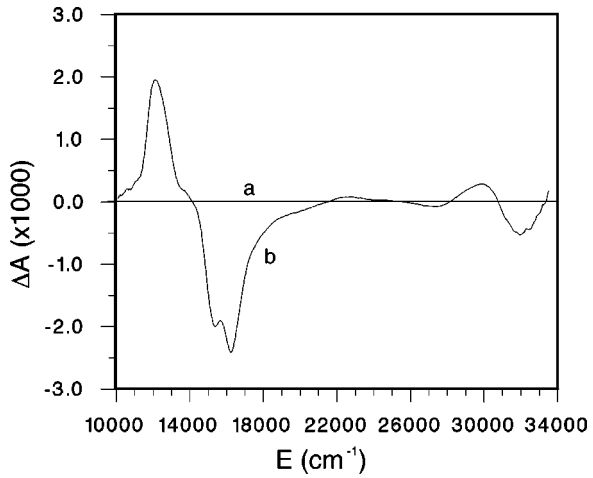

FIG. 4. MCD spectra at 1.4 K and 2.5 T of Rh^{2+} in a Rh^{3+}-doped NaCl solution-grown crystal for the magnetic field and incident circularly polarized light parallel to $\langle 100\rangle$. Curve *a* shows the MCD spectrum of the nontreated Rh^{3+}-doped NaCl, and curve *b* is the MCD spectrum of the crystal *x*-ray irradiated at 77 K and after a long anneal at room temperature.

it was kept for at least a day. After such treatment and after subtraction of the absorption of the untreated crystal, a new strong band in the 29 000–30 000 cm^{-1} is readily detected (Fig. 3). This procedure was repeated several times to enhance the signal intensity. Using the suggested background in this figure, it is clear that the intensity of the two $d-d$ transitions of Rh^{3+} has been reduced by roughly 25%, indicating the formation of either Rh^{4+} or Rh^{2+}, both of which are paramagnetic. In ESR only Rh^{2+} complexes are detected. At the same time the difference spectrum shows the presence of a small absorption around 16 000 cm^{-1}. The corresponding differential absorption dA is at most 3×10^{-3}. Sensitive MCD measurements turn out to be essential for its identification and correlation with the Rh^{2+} ESR data.

It is also clear from Figs. 2 and 3 that irradiation causes a decrease of the absorbance beyond 31 000 cm^{-1}. This is consistent with the expected manifestation in this spectral region of a reduction in intensity of the charge transfer band of Rh^{3+}.

Crystals that were annealed to 500–700 °C show an optical absorption spectrum similar to the *x*-irradiated crystals kept a long time at room temperature. However, the optical spectra are superimposed on a large background due to scattering from small inclusions produced by the heat treatment. This opaqueness makes the crystals quite unsuitable for optical experiments in the near uv and we have found no discernible optical absorption band in the 19 350 cm^{-1} region as reported in Ref. 9.

C. Magnetic circular dichroism

The MCD spectra of NaCl:Rh^{3+} were taken before *x* irradiation and a long time after *x*-irradiation and storage at room temperature. In this way the dominant MCD spectra represent the RTAX Rh^{2+} related features. Figure 4 demonstrates that the nonirradiated crystal exhibits no MCD, in agreement with the absence of ESR signals before irradiation. By contrast, the *x*-irradiated crystal shows large positive and negative MCD signals at $(12\,200\pm50)$ cm^{-1} and $(16\,200\pm50)$ cm^{-1}, respectively, together with additional features at higher energies beyond 26 000 cm^{-1}, and an extra peak at $(15\,350\pm50)$ cm^{-1}. These numbers are summarized in Table II. The strongest MCD signal at 16 200 cm^{-1} and at 3 T is of strength $\Delta A=2.2\times10^{-3}$, where ΔA is the differential absorbance for left (σ_+) and right (σ_-) circularly polarized light. This signal is only slightly weaker than the absorbance at 16 000 cm^{-1} created by *x* irradiation (Fig. 2). It is reasonable to assign the weak 16 000 cm^{-1} absorption to the dominant MCD signal in this region. The additional peak at $(15\,350\pm50)$ cm^{-1} partially disappears a very long time after *x* irradiation.

TABLE II. Optical absorption and MCD data for the $Rh^{2+}(4d^7)$ complex in solution-grown NaCl:Rh^{2+}. The terms between brackets are the parentage terms of Rh^{3+}.

Center	Transition (O_h notation)	Absorption maximum (cm^{-1})
Rh^{2+}(RTAX,D_{4h})	$^2E_g\rightarrow{}^2T_{1g}(^3A_2)$ $^2E_g\rightarrow{}^2T_{2g}(^1E)\}$	$12\,200\pm50$
Rh^{2+}(RTAX,D_{4h})	$^2E_g\rightarrow{}^2T_{1g}(^1E)$ $^2E_g\rightarrow{}^2T_{2g}(^1A_1)\}$	$16\,200\pm50$
Rh^{2+} (B center) [a]	$^2E_g\rightarrow{}^2T_{1g}(^3A_2)$ $^2E_g\rightarrow{}^2T_{2g}(^1E)\}$	$\sim12\,200$
Rh^{2+} (B center) [a]	$^2E_g\rightarrow{}^2T_{1g}(^1E)$ $^2E_g\rightarrow{}^2T_{2g}(^1A_1)\}$	$15\,350\pm50$
Rh^{2+}	charge-transfer	$\sim29\,500$

[a]Tentatively associated with a Rh^{2+} center in which one of the six Cl^- ligands is exchanged with either OH^- or H_2O (Ref. 3).

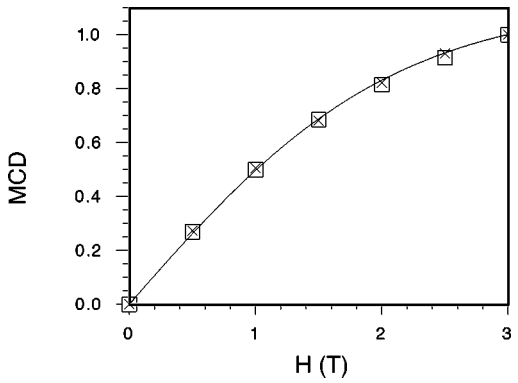

FIG. 5. MCD saturation curves at 1.4 K as a function of magnetic field H between 0 T and 3 T. The MCD signal is defined as MCD(H)/MCD(3 T). The squares represent the saturation of the band at 12 200 cm^{-1} and the crosses of the band at 16 200 cm^{-1}. The line is the calculated Brillouin function for a spin $S=1/2$ and a Landé factor of 2 (see text).

The saturation of the MCD at 16 200 cm^{-1} as a function of the magnetic field at 1.4 K, has been measured carefully and is shown in Fig. 5. Similar results were found with the monochromator set at 12 200 cm^{-1}. Saturation measurements were not meaningful at 30 000 cm^{-1} because of poor signal-to-noise ratio. For the two bands at lower energies, the MCD field dependence of the saturation follows a Brillouin function $\tanh(g\mu_B H/2k_B T)$ for electron spin $S=1/2$ and $g\approx 2$. The data points are found very close to the calculated curve. These results support our conclusion that we are dealing with MCD signals originating from the RTAX Rh^{2+} center.

IV. DISCUSSION

The ground state for the Rh^{2+} ion in an octahedral field with O_h symmetry is ${}^2E_g(t_{2g}^6 e_g^1)$. For the Rh^{2+} RTAX center a decrease in symmetry, $O_h \rightarrow D_{4h}$, has occurred as a result of a Jahn-Teller distortion together with, or induced by, molecular binding with the two equivalent chloride ions. This results in either a ${}^2A_{1g}(e_g^4 b_{2g}^2 a_{1g}^1)$ or ${}^2B_{1g}(e_g^4 b_{2g}^2 b_{1g}^1)$ ground state. The analysis of the ESR data establishes, in agreement with earlier work, that ${}^2A_{1g}$ is the ground state. The D_{4h} electronic configuration can be looked upon either as a strong field split atomic d^7 configuration of the Rh^{2+} ion or as the molecular configuration of a $RhCl_2$ molecule which is the dominant part of the Rh^{2+} RTAX center.

In either viewpoint expressions for the **g** matrix components can be calculated. Using linear combinations of three hole wave functions to describe the Rh^{2+} terms derived from the strong field split d^7 configuration and by mixing the excited states through spin-orbit interaction the following expressions have been obtained for the ${}^2E_g({}^2A_{1g})$ ground state:[15]

$$g_\parallel = g_0 + 4k\xi\left(-\frac{1}{\Delta_3}+\frac{1}{\Delta_1}\right),$$
$$g_\perp = g_0 + k\xi\left(\frac{1}{\Delta_3}-\frac{1}{\Delta_1}+\frac{3}{\Delta_2}+\frac{3}{\Delta_4}\right), \quad (2)$$

with $g_0=2.0023$, ξ the matrix element of the the spin-orbit interaction between the ground state and the excited states, k the orbital reduction factor, and Δ_1, Δ_2, Δ_3, and Δ_4, the energy difference of the $t_{2g}^6 e_g^1$ ground state ${}^2E_g({}^2A_{1g})$ with the $t_{2g}^5 e_g^2$ excited states,[15] ${}^2T_{1g}({}^3A_{2g})$, ${}^2T_{2g}({}^1E_g)$, ${}^2T_{1g}({}^1E_g)$, and ${}^2T_{2g}({}^1A_{1g})$, respectively. The states between brackets are the parentage states of the Rh^{3+} ion.[16] No attempt was made to expand expressions (2) to D_{4h} symmetry. Since one would expect a multitude of transitions in such a case whereas only two main bands are observed, the energy splittings in D_{4h} are probably too small to be measurable, and most likely they are small compared to the energy differences in the denominators of the g factor formulas (2).

Expressions (2) are quite adequate to perform the following quantitative analysis. In a purely atomic approximation of the Rh^{2+} RTAX center one can use[14] $\xi=1235$ cm^{-1}. Only two MCD absorptions are observed and we will assume that these are the only resolved ones. Substituting several possible combinations of the absorption values for $\Delta_{1,2,3,4}$ in expressions (2) yields indeed only a good fit for the choice $\Delta_1\approx\Delta_2\approx 12\,200$ cm^{-1}, and $\Delta_3\approx\Delta_4\approx 16\,200$ cm^{-1}. Using $k=0.89$, we obtain 2.451 and 2.024 for $g_\perp$, $g_\parallel$, respectively. The accuracy of the calculated g values, or of the Δ_i values for that matter, is here and below primarily determined by the accuracy by which the product $k\xi$ is known. From the MCD absorption values the Racah B parameter can be estimated: the energy difference between the two ${}^2E_g \rightarrow {}^2T_{1g}$ transitions yields $8B$, which gives $B=500$ cm^{-1}. Furthermore, from the lowest ${}^2E_g \rightarrow {}^2T_{1g}$ transition the crystal field splitting $10Dq$ can be estimated to be about 14 000 cm^{-1}.

It may be noted that expressions (2) can explain the observed small positive shift for $g_\parallel$ (Table I), while expressions derived within a purely configurational approximation cannot:[2,14,17,18] $g_\perp = g_0 + 6\xi/\Delta_{1,3}$ and $g_\parallel = g_0$, with $\Delta_{1,3}$ the energy difference between $t_{2g}^6 e_g^1$ and $e_{2g}^5 e_g^2$. It has been suggested[14,6] that a vibronically induced admixture of B_{1g} (in D_{4h} notation) into the A_{1g} ground state may yield a positive contribution to $g_\parallel$. The g factor for a pure B_{1g} ground state leads to g components which behave as $g_\parallel > g_\perp > g_0$.[15] On the basis of these results we estimate that a very small mixture, at most 3%, of b_{1g} into a_{1g} would be sufficient to account for the positive $g_\parallel$ shift.[6] Barring new information, expressions (2) are to be preferred at this point.

The analysis of the ESR parameters makes it reasonable to assign the MCD absorption at 12 200 cm^{-1} to two nonresolved ${}^2E_g \rightarrow {}^2T_{1g}, {}^2T_{2g}$ transitions, and analogously 16 200 cm^{-1} to two higher energy nonresolved ${}^2E_g \rightarrow {}^2T_{1g}, {}^2T_{2g}$ transitions, listed in Table II. These are parity forbidden but become weakly vibronically allowed by mixing of odd states through odd vibrational modes.

The 15 350 cm^{-1} band can be assigned to an optical transition from the ESR B spectrum mentioned earlier, and probably is of the same origin as the 16 200 cm^{-1} band, i.e., ${}^2E_g \rightarrow {}^2T_{1g}, {}^2T_{2g}$. The two lower bands must then be coincident with the two low energy transitions at 12 200 cm^{-1} of the RTAX center. With the same expression (2) the g values of the B spectrum can be calculated: 2.466 and 2.021, for $g_\perp$ and $g_\parallel$, respectively. The calculated $g_\perp$ value is shown in Fig. 1. It agrees quite well with the experimental value.

Our ESR correlated MCD and optical absorption data do not agree with the optical absorption result for Rh^{2+} presented in Ref. 9. We do not detect an optical absorption around 19 350 cm^{-1} and, more importantly, the MCD spectrum shows no paramagnetic band of reasonable intensity at this energy. In Ref. 9, the crystals were annealed to 500–600 °C which produced a high density of macroscopic optical scattering inclusions and resulted in samples of poor optical quality. Our ESR analysis has shown that after such a thermal anneal the dominant species is the O(II) Rh^{2+} center. In view of the small orthorhombicity of the **g** matrix of O(II) and the very comparable $g_{\perp}$ values (Table I), it is likely that very little difference, if any, should be observable between the optical absorption spectra of O(II) and RTAX Rh^{2+} centers.

Although it is quite straightforward to identify the RTAX optical absorption signals at 12 200 cm^{-1}, 16 200 cm^{-1}, by MCD and ESR, no such tools exist for the strong absorption band at 29 500 cm^{-1} (Fig. 3). Since the formation of this band broadly parallels the formation of the ESR signal of the Rh^{2+} center it is not unlikely that this band is related to a rhodium center, i.e., Rh^{2+}, Rh^{+} or Rh^{0}, the latter two produced by the subsequent trapping of electrons by the Rh^{2+} RTAX center. Rh^{0} is not observed in the ESR spectra, so this possible assignment is not considered. Another possibility is the Rh^{+} center. The existence of such a center is not unreasonable because the Rh^{2+} RTAX is not charge compensated by a cation vacancy and still possesses a Coulomb attraction for another electron. The presence of Rh^{+} ions in solution-grown NaCl crystals after similar treatments, has recently been established.[20] However the charge-transfer spectrum of the Rh^{+} center would consist of one allowed $^3A_{2g} \rightarrow {}^3T_{2u}$ transition, split by spin-orbit interaction into three components. This is not observed in either MCD or optical absorption, so the Rh^{+} assignment should also be rejected. The only possibility left are the charge transfer bands of Rh^{2+}, i.e., the allowed $^2E_g \rightarrow {}^2T_{1u}, {}^2T_{2u}$ transitions, which both are split into two spin-orbit components. It can be shown that the polarizations of both transitions are inverted for each of the spin-orbit (E' and U') components, so that both σ_+ and σ_--type of transitions are of equal magnitude, but opposite sign. This explains the smallness of the observed MCD signal.

Unfortunately, the sign of the MCD signals cannot be established for the ligand field bands of Rh^{2+}. Although the appropriate procedure has long been established in the case of vibronically assisted bands,[19] the model requires too many unknown parameters to make the prediction reliable.

Finally, we have, as is customary in the field of transition metal ions, assigned the optical absorptions within the framework of the octahedral Tanabe-Sugano formalism for the Rh^{2+}, even though the ESR results clearly establishes D_{4h} symmetry for the center together with a $RhCl_2$ molecule as its essential core. One must conclude that the electronic correlation effects within the Rh^{2+} ion still dominate the energy splittings within the molecule and that covalency effects with the two chlorines play a minor role.

V. CONCLUSIONS

Through the combined application of optical absorption, electron spin resonance, and magnetic circular dichroism techniques to *x*-irradiated solution-grown NaCl:Rh^{3+} we have been able to correlate two intense paramagnetic absorption bands at 12 200 cm^{-1} and 16 200 cm^{-1} and an absorption around 30 000 cm^{-1}, to a paramagnetic Rh^{2+} complex. A quantitative analysis of the **g** matrix components makes it reasonable to assign the vibronically allowed 12 200 cm^{-1} and 16 200 cm^{-1} MCD absorptions to transitions from the $^2E_g(^2A_{1g})$ ground state to two distinct pairs[10] of $^2T_{1g,2g}$ excited states within the Rh^{2+} complex. Tentative assignments for the other two absorption features have also been presented.

ACKNOWLEDGMENTS

The authors H.V. and F.C. are indebted for financial support to the *Flemish Institute for the Encouragement of the Scientific and Technological Research in the Industry (IWT)* and the *Fund for Scientific Research, Flanders (FWO)*, respectively. This work was supported in part by Agfa-Gevaert NV (Mortsel) and by IWT. The authors want to thank H. Bou Rjeily for his help with the MCD experiments.

[1] H. Vercammen, T. Ceulemans, D. Schoemaker, F. Callens, and D. Vandenbroucke, J. Appl. Phys. **84**, 428 (1998).
[2] J. R. Shock and M. T. Rogers, J. Chem. Phys. **62**, 2640 (1975).
[3] M. Zdravkova, H. Vrielinck, F. Callens, E. Boesman, H. Vercammen, and D. Schoemaker, J. Appl. Phys. **82**, 2476 (1997).
[4] M. T. Olm, J. R. Niklas, J. M. Spaeth, and M. C. R. Symons, Phys. Rev. B **38**, 4343 (1988).
[5] S. Schweizer and J.-M. Spaeth, J. Phys. Chem. Solids **58**, 859 (1997).
[6] H. Vercammen, D. Schoemaker, H. Käß, E. Goovaerts, A. Bouwen, H. Vrielinck, and F. Callens, J. Appl. Phys. **84**, 428 (1998).
[7] F. Callens, M. Zdravkova, H. Vrielinck, P. Matthys, H. Vercammen, and D. Schoemaker, J. Appl. Phys. **84**, 422 (1998).
[8] C. K. Jørgensen, Acta Chem. Scand. **10**, 500 (1956).
[9] C. Görller-Walrand, B. Gilliams, and J. D'Olieslager, Chem. Phys. Lett. **246**, 163 (1995).
[10] Y. Tanabe and S. Sugano, J. Phys. Soc. Jpn. **9**, 753 (1954).
[11] E. Moya, C. Zaldo, B. Briat, V. Topa, and F. J. Lopez, J. Phys. Chem. Solids **54**, 809 (1993).
[12] D. Schoemaker, Phys. Rev. B **7**, 786 (1973).
[13] W. B. Fowler, *Physics of Color Centers* (Academic Press, New York, 1968), Appendix B.
[14] A. Abragam and B. Bleaney, *Electron Paramagnetic Resonance of Transition Ions* (Clarendon, Oxford, 1970).
[15] M. G. Townsend, J. Chem. Phys. **41**, 3149 (1964).
[16] J. S. Griffith, *The Theory of Transition Metal Ions* (Cambridge

University Press, Cambridge, England, 1971).
[17] A. H. Maki, N. Edelstein, A. Davidson, and R. H. Holm, J. Am. Chem. Soc. **86**, 4580 (1964).
[18] R. P. Muniz, N. V. Vugman, and J. Danon, J. Chem. Phys. **54**, 1284 (1971).
[19] M. J. Harding and B. Briat, Mol. Phys. **25**, 745 (1973).
[20] H. Vrielinck, F. Callens, M. Zdravkova, and P. Matthys, J. Chem. Soc. Faraday Trans. **94**, 2999 (1998).